

Doubly-Generalized LDPC Codes with SPC Codes as Super Variable Nodes

Yejun He, Jie Yang and Guiyuan Sun

Shenzhen Key Lab of Media Security, Shenzhen Key Lab of Advanced Communications and Information Processing
College of Information Engineering, Shenzhen University, 518060, China
Email: {heyejun, yangjie8925, sunguiyuan66}@126.com

Abstract—In this paper, we design and analyze three kinds of doubly-generalized low-density parity-check (D-GLDPC) codes. We employ single parity-check (SPC) codes as super variable nodes (SVNs) and two-dimensional (2-D) single parity-check product codes (SPC-PCs) as super check nodes (SCNs). Three kinds of different SPC codes as super variable nodes (SVNs) are used in the systematic (*S*) form, the cyclic (*C*) form and the anti-systematic (*A*) form. Because the minimum distance of SPC codes is 2, they can meet upper bound of D-GLDPC codes. The performance of the proposed D-GLDPC codes is investigated over the AWGN channel with the extrinsic information transfer (EXIT) charts. The SPC codes in different forms have an effect on stability bound of D-GLDPC codes and also make a difference in decoding threshold. Simulation results show that D-GLDPC codes with *C*-form SPC codes as SVNs have the best stability bound and the minimum decoding threshold, the second best is D-GLDPC codes with *S*-form SPC codes as SVNs, and the worse one is D-GLDPC codes with *A*-form SPC codes as SVNs.

I. INTRODUCTION

LDPC codes were first proposed by Gallager in [1] and later rediscovered by MacKay and Neal [2]. A LDPC code can be represented as a bipartite graph, also known as Tanner graph. They are divided into two disjoint set, namely, the variable nodes (VNs) and the check nodes (CNs). The traditional LDPC codes can be regarded as SPC codes at the CNs and repetition codes (RCs) at the VNs. If all VNs have the same degree distributions and all CNs have the same degree distributions, the code is called regular LDPC code, otherwise it is called irregular LDPC code. Irregular LDPC codes were introduced in [3], and were shown to have better performance than regular LDPC codes over the binary erasure channel (BEC). They employ iterative message passing (BP) decoding algorithm. By replacing SPC codes and repetition codes with generic linear block codes, D-GLDPC codes are formed [4]. Simultaneously the VNs become super variable nodes (SVNs), and the CNs become super check nodes (SCNs). If only the SPC codes are generalized, while the repetition codes remain unchanged, then the codes are generalized LDPC (GLDPC) codes [5].

In a D-GLDPC code, the codes used as SVNs and SCNs are called component codes. i.e., variable component codes and check component codes. For example, Hamming check component codes have been proposed in [6]. The analysis of weight distribution of Bose-Chaudhuri-Hocquenghem (BCH) check component codes has been introduced in [7]. [8] investigates irregular VNs and uniform SCNs, where SCNs are constrained with Hadamard codes. All these constructions are

based on strengthening the check component codes at the cost of reducing code rate. In order to analyze D-GLDPC codes, extrinsic information transfer (EXIT) charts over the AWGN channel have been used in [9], [10].

SPC codes at SVNs exhibit excellent characteristics. Firstly, they can make up for the code rate loss of length-*n* repetition code. Secondly, their minimum distances are 2, which makes them to compensate for the area gap between the EXIT curves. Finally, they are easy to decode. In this paper, we use three different forms of SPC codes as SVNs and apply EXIT chart to analyze the stability bound and decoding threshold of D-GLDPC codes since stability bound is an upper bound on the iterative decoding threshold [11]. The SPC codes used by us possess different generator matrices. When the minimum distance of generator matrices $d_{min} = 2$ [12], SPC codes contribute to the stability bound. Meanwhile, we make use of EXIT chart to optimize the degree distributions of our D-GLDPC codes, and analyze curve matching of three kinds of SPC codes with various forms.

The rest of the paper is organized as follows. In section II, we recall the main definitions related to D-GLDPC codes and introduce SPC codes in different representations. An analysis of stability bound and EXIT chart are in Section III. Several examples and results are presented in Section IV and the conclusions are summarized in Section V.

II. CODE STRUCTURE

A. D-GLDPC Codes

The Tanner graph of D-GLDPC codes can be obtained from that of LDPC codes with VNs and CNs replaced by SVNs and SCNs, respectively. Fig. 1 shows the Tanner graph of a D-GLDPC code with *M* SCNs and *N* SVNs. We refer to the parity-check matrix of the LDPC code as the base matrix. The size of the base matrix is $M \times N$.

For the *j*-th SVN ($j = 1, 2, \dots, N$), the component code is represented by $(n_{v,j}, k_{v,j})$, which means that $n_{v,j}$ coded bits are formed for every $k_{v,j}$ information bits. Similarly, for the *i*-th SCN ($i = 1, 2, \dots, M$), the component code is denoted by $(n_{c,i}, k_{c,i})$. We denote the check component code associated with the *i*-th SCN by C_i , and the variable component code associated with the *j*-th SVN by V_j . Thus the size of parity-check matrix of C_i is given by $m_{c,i} \times n_{c,i}$ (where $m_{c,i} < n_{c,i} - k_{c,i}$, if redundant rows in check equations exist; $m_{c,i} = n_{c,i} - k_{c,i}$, otherwise) and the size of generator matrix of V_j

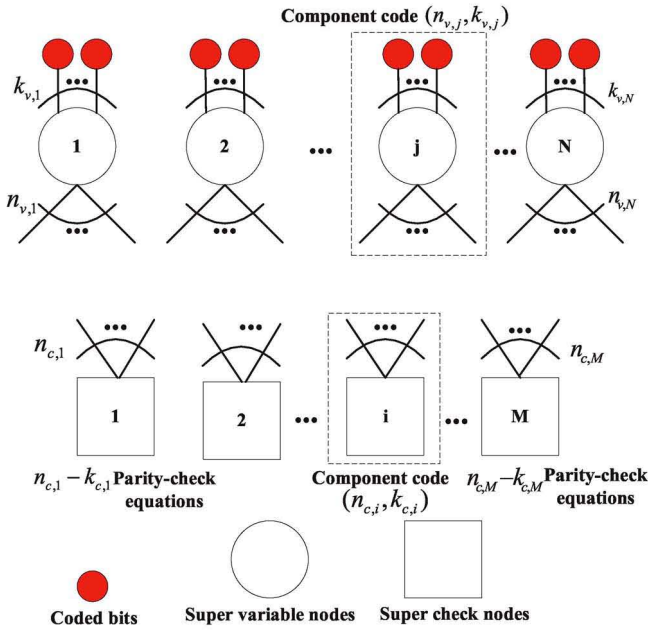


Fig. 1. The bipartite graph of a D-GLDPC code

given by $k_{v,j} \times n_{v,j}$. The overall code rate of the D-GLDPC code meets

$$R = 1 - \frac{\sum_{i=1}^M m_{c,i}}{\sum_{j=1}^N k_{v,j}} \geq 1 - \frac{\sum_{i=1}^M (n_{c,i} - k_{c,i})}{\sum_{j=1}^N k_{v,j}} \quad (1)$$

The parity-check matrix of a D-GLDPC code can be obtained from its base matrix with row expansion and column expansion [4].

B. Three kinds of SPC codes at SVNs

Assuming that the type- i SVNs are $(n_i, n_i - 1)$ SPC codes in systematic form, its generator matrix is

$$\mathbf{G}_S^i = \begin{pmatrix} 1 & 0 & 0 & \cdots & 0 & 1 \\ 0 & 1 & 0 & \cdots & 0 & 1 \\ 0 & 0 & 1 & \cdots & 0 & 1 \\ \vdots & \vdots & \vdots & \ddots & \vdots & \vdots \\ 0 & 0 & 0 & \cdots & 1 & 1 \end{pmatrix}_{(n_i-1) \times n_i} \quad (2)$$

For these SVNs, each one has $\binom{n_i}{2}$ weight-2 codewords. There are $n_i - 1$ weight-2 codewords produced by weight-1 information words, and $\binom{n_i-1}{2}$ weight-2 codewords produced by weight-2 information words. No other larger than 2 information words generate weight-2 codewords. Let $B_{2,u}^i$ denote the number of Hamming weight-2 codewords that generalized by Hamming weight- u for type- i SVNs. Thus we can obtain $B_{2,u}^i$ of SPC codes in systematic form by [12].

$$B_{2,u}^i = \begin{cases} n_i - 1 & u = 1 \\ \binom{n_i-1}{2} & u = 2 \\ 0 & u = 3, \dots, n_i - 1 \end{cases} \quad (3)$$

Assuming that the type- i SVNs are $(n_i, n_i - 1)$ SPC codes in cyclic form, its generator matrix is represented by

$$\mathbf{G}_C^i = \begin{pmatrix} 1 & 1 & 0 & \cdots & 0 & 0 \\ 0 & 1 & 1 & \cdots & 0 & 0 \\ 0 & 0 & 1 & \cdots & 0 & 0 \\ \vdots & \vdots & \vdots & \ddots & \vdots & \vdots \\ 0 & 0 & 0 & \cdots & 1 & 1 \end{pmatrix}_{(n_i-1) \times n_i} \quad (4)$$

$B_{2,u}^i$ in cyclic form is given by [12]

$$B_{2,u}^i = n_i - u \quad u = 1, \dots, n_i - 1 \quad (5)$$

Let us suppose the SVNs of type- i are $(n_i, n_i - 1)$ SPC codes in anti-systematic form. In this case, n_i is odd. Since for even n_i , we obtain a weight-1 codewords when encoding it, this situation is not allowed. The generator matrix of SPC codes in anti-systematic form is obtained from the generator matrix in systematic form by adding one bit in first $n_i - 1$ columns. Thus the generator matrix of SPC codes in anti-systematic form can be written as

$$\mathbf{G}_A^i = \begin{pmatrix} 0 & 1 & 1 & \cdots & 1 & 1 \\ 1 & 0 & 1 & \cdots & 1 & 1 \\ 1 & 1 & 0 & \cdots & 1 & 1 \\ \vdots & \vdots & \vdots & \ddots & \vdots & \vdots \\ 1 & 1 & 1 & \cdots & 0 & 1 \end{pmatrix}_{(n_i-1) \times n_i} \quad (6)$$

According to the definition of $B_{2,u}^i$, we derive $B_{2,u}^i$ of SPC codes in anti-systematic form as follows

$$B_{2,u}^i = \begin{cases} \binom{n_i-1}{2} & u = 2 \\ n_i - 1 & u = n_i - 2 \\ 0 & u = 3, \dots, n_i - 3 \end{cases} \quad (7)$$

III. ASYMPTOTICS

A. Stability Bound

Let us consider a D-GLDPC code with $(n_i, n_i - 1)$ SPC codes at SVNs. According to [12], $P_i(x)$ is defined as follows

$$P_i(x) = \sum_{u=1}^{n_i-1} \frac{2B_{2,u}^i}{n_i} x^u \quad (8)$$

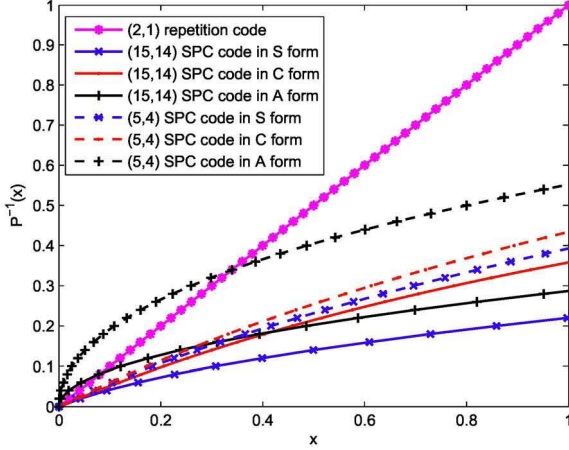
For the SPC codes in systematic and cyclic form, $P_i(x)$ has been given in [12], we denote them by $P_i^S(x)$ and $P_i^C(x)$, and rewrite them as follows

$$P_i^S(x) = \frac{2(n_i - 1)}{n_i} x + \frac{(n_i - 1)(n_i - 2)}{n_i} x^2 \quad (9)$$

$$P_i^C(x) = \sum_{u=1}^{n_i-1} \frac{2(n_i - u)}{n_i} x^u \quad (10)$$

For the SPC codes in anti-systematic form, we use (7) to substitute $B_{2,u}^i$ in (8), then $P_i^A(x)$ becomes

$$P_i^A(x) = \frac{(n_i - 1)(n_i - 2)}{n_i} x^2 + \frac{2(n_i - 1)}{n_i} x^{n_i-2} \quad (11)$$

Fig. 2. $P^{-1}(x)$ of SPC codes in different forms for a D-GLDPC code

We define $P^{-1}(x)$ as the inverse function of $P_i(x)$. If $n_i = 3$, according to (9), (10) and (11), we obtain

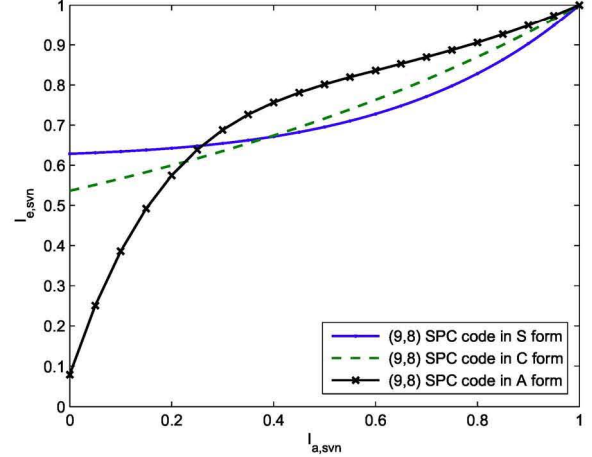
$$P_i^S(x) = P_i^C(x) = P_i^A(x) = \frac{2}{3}x^2 + \frac{4}{3}x \quad (12)$$

So it is equal to $P^{-1}(x)$ in three forms when $n_i = 3$. For $n_i > 3$, we plot $P^{-1}(x)$ against x in Fig. 2. We denote systematic form by S , cyclic form by C and anti-systematic form by A . From Fig. 2, we can see $P^{-1}(x)$ in A form and $P^{-1}(x) = x$ ($P(x)$ of length-2 repetition code is x) intersect at $x \in (0, 1)$, which will be proved in the APPENDIX. Since the intersection contributes to the stability bound, the decoding threshold increases substantially comparing to the other two. We also know that SPC codes in C form has a better potential comparing to SPC codes in S form. The SPC codes in C form provide a lower threshold E_b/N_0 when $0 < x < 1$.

B. EXIT Chart Analysis

The EXIT chart can be used to analyze the convergence behavior of decoders [13]. For a D-GLDPC code, the EXIT chart includes two curves: they correspond to the SVN decoders and SCN decoders, respectively. Each EXIT curve shows the relationship between the a priori information and the extrinsic information of the component decoder by tracking the mutual information. For a D-GLDPC code, the closed-form EXIT functions of SVN types and SCN types over the binary erasure channels (BECs) have been derived in [12].

We assume that both the communication channel and the extrinsic channel are BECs, and their erasures probabilities are q and p , respectively. For a general (n_v, k_v) component code at SVN, the closed-form EXIT function over the BEC is given by [12]. If $(n_i, n_i - 1)$ SPC codes are used as SVNs, by replacing

Fig. 3. EXIT curves of (9,8) SPC codes in S form, C form and A form

$1 - p$ with $I_{a,svn,spc}^{BEC}$, the EXIT function can be rewrite as

$$\begin{aligned} I_{e,svn,spc}^{BEC}(I_{a,svn,spc}^{BEC}, q) = 1 - \frac{1}{n_i} \sum_{t=0}^{n_i-1} \sum_{z=0}^{n_i-1} & (1 - I_{a,svn,spc}^{BEC})^t \\ & \cdot (I_{a,svn,spc}^{BEC})^{n_i-t-1} \cdot q^z (1-q)^{n_i-z-1} \\ & \cdot [(n_i - t)\tilde{e}_{n_i-t, n_i-z-1} - (t+1)\tilde{e}_{n_i-t-1, n_i-z-1}] \end{aligned} \quad (13)$$

where $\tilde{e}_{g,h}$ is named as the (g, h) -th split information function and is defined as the summation of the ranks of all the possible sub-matrices obtained by choosing g column(s) in the corresponding $(n_i - 1) \times n_i$ generator matrix and h column(s) in the corresponding $(n_i - 1) \times (n_i - 1)$ identity matrix. By transforming $q = 1 - J(\sqrt{8 \cdot R \cdot 10^{E_b/N_0}/10})$ [13], we can obtain approximate EXIT functions over the AWGN channel, where R is the code rate of the D-GLDPC code and $J(\cdot)$ is defined in the appendix of [14]. $\tilde{e}_{g,h}$ for SPC codes in different forms are different, so there is a big difference among the EXIT functions. Fig. 3 shows the EXIT curves at SVNs using SPC codes in S form, C form and A form, where $R = 0.6$ and $E_b/N_0 = 1.943$ dB.

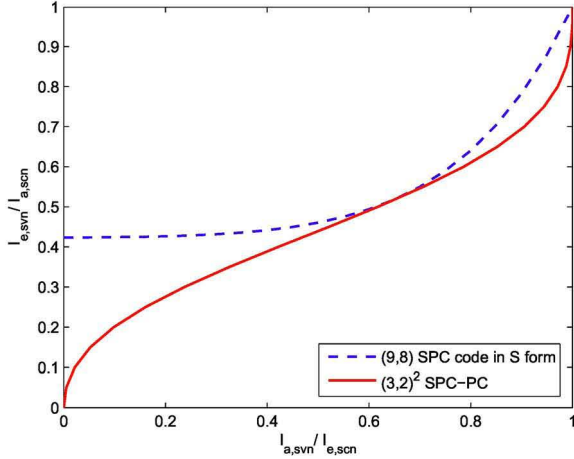
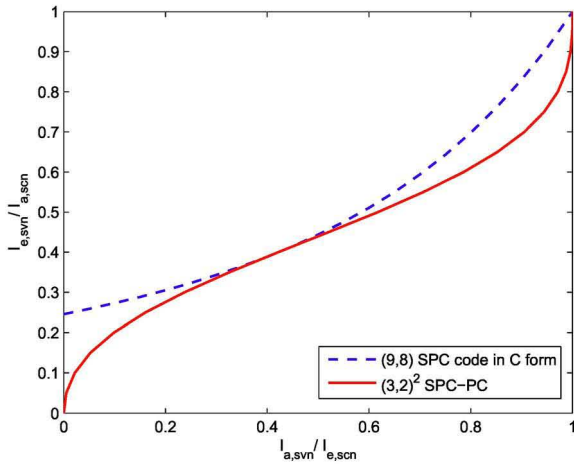
For a general (n_c, k_c) constituent code used as SCN, the EXIT function is given by [12]. By replacing $1 - p$ with $I_{a,scn}^{BEC}$, we obtain

$$\begin{aligned} I_{e,scn}^{BEC}(I_{a,scn}^{BEC}) = 1 - \frac{1}{n_c} \sum_{t=0}^{n_c-1} & (I_{a,scn}^{BEC})^{n_c-t-1} (1 - I_{a,scn}^{BEC})^t \\ & \cdot [(n_c - t)\tilde{e}_{n_c-t} - (t+1)\tilde{e}_{n_c-t-1}] \end{aligned} \quad (14)$$

where \tilde{e}_g is named as the g -th information function and is defined as the summation of the ranks of all the possible sub-matrices obtained by choosing g column(s) in the corresponding $k_c \times n_c$ generator matrix.

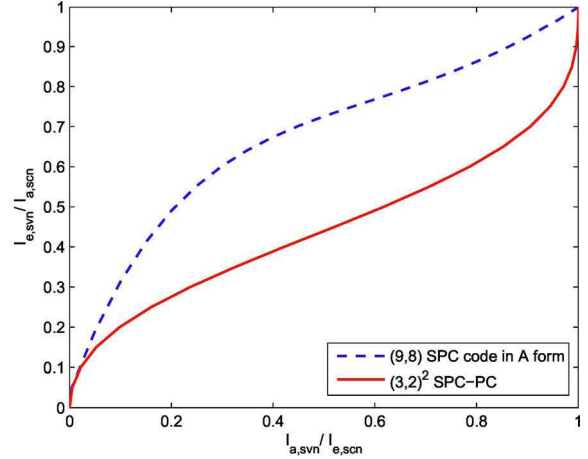
IV. EXAMPLES AND RESULTS

We use $(n, n-1)^2$ single parity-check product codes (SPC-PCs) at SCNs. Since the minimum distance of a 2-D SPC-PC

Fig. 4. EXIT chart of $(3, 2)^2$ SPC-PC and $(9, 8)$ SPC code in S formFig. 5. EXIT chart of $(3, 2)^2$ SPC-PC and $(9, 8)$ SPC code in C form

is $d_{min} = 2^2 = 4$ [15], the SPC-PC can reduce interference of the codewords. In Fig. 4, Fig. 5 and Fig. 6, we employ $(3, 2)^2$ SPC-PCs as SCNs and $(9, 8)$ SPC codes as SVN s , and plot the EXIT fitting of SPC-PC and SPC code in different forms. From these figures, we observe that an area gap between two curves is minimum in Fig. 5. The smaller the area gap is, the smaller the decoding threshold is. TABLE I lists some results about code rate and decoding threshold. As seen from TABLE I, we found that for the same codes, the higher the code rate, the higher the decoding threshold. For codes in different forms, when they have same code rate, we found that SPC codes in C form has the minimum threshold. In order to be compatible with code rate and the threshold, we should choose good codes with a higher code rate and a lower threshold in an actual communication system.

In order to compensate for the area gap, we optimize the degree distribution of the D-GLDPC codes. Fig. 7, Fig. 8 and

Fig. 6. EXIT chart of $(3, 2)^2$ SPC-PC and $(9, 8)$ SPC code in A formTABLE I
DECODING THRESHOLD FOR DIFFERENT CODE TYPES

Code type	Code rate	Threshold(dB)		
		S	C	A
$(3, 2)^2$ SPC-PC + $(9, 8)$ SPC	0.375	1.114	0.727	1.726
$(3, 2)^2$ SPC-PC + $(7, 6)$ SPC	0.352	0.924	0.611	1.655

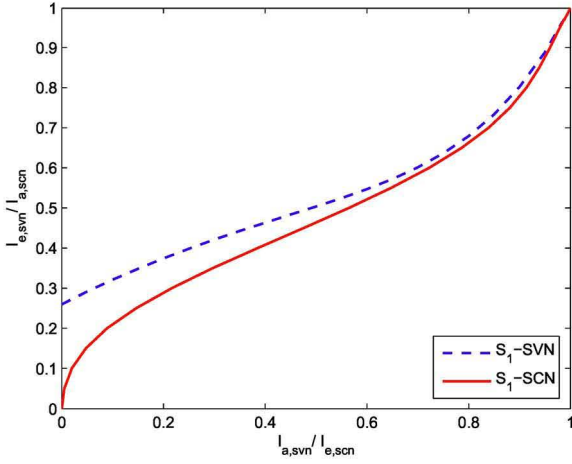
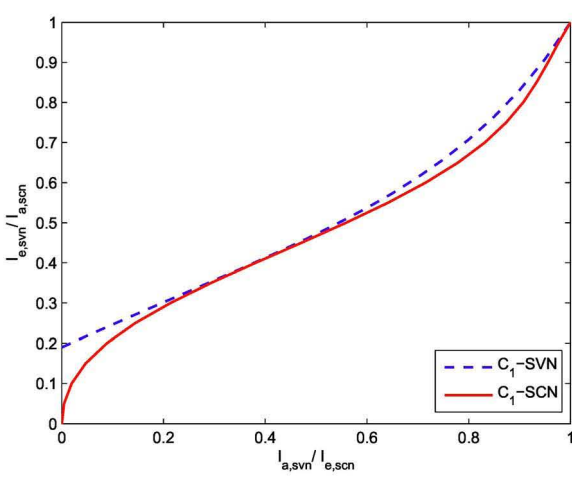
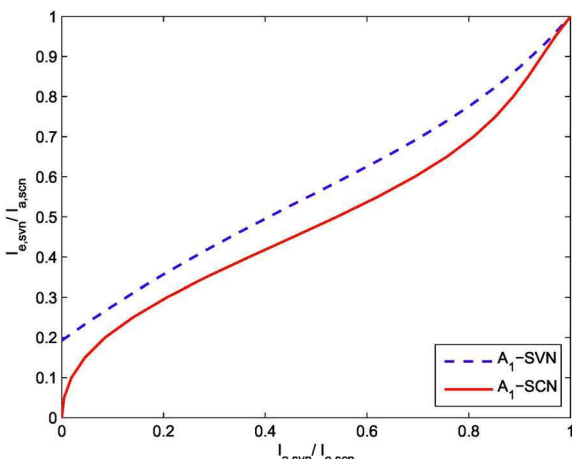
Fig. 9 are the EXIT charts for our D-GLDPC codes whose degree distributions are shown in TABLE II. In the three columns of TABLE II, we label “D-GLDPC S_1 ”, “D-GLDPC C_1 ” and “D-GLDPC A_1 ” as the optimization of the D-GLDPC ensembles using the SPC as SVN s in systematic, in cyclic form and anti-systematic form, respectively. In this case we fix decoding threshold to 0.141 dB. The area gap of D-GLDPC codes with anti-systematic form SPC code is the largest and the area gap of D-GLDPC codes with cyclic form SPC code is the smallest, which illustrates the decoding threshold of D-GLDPC codes with SPC codes in cyclic form is the best and the decoding threshold of D-GLDPC codes with SPC codes in anti-systematic form is the worst.

V. CONCLUSIONS

In this paper, we employed three kinds of different SPC codes as SVN s in D-GLDPC codes. We discussed the stability bound of these D-GLDPC codes, and used EXIT chart to

TABLE II
OPTIMUM DEGREE DISTRIBUTIONS OF OUR D-GLDPC CODES

	D-GLDPC S_1	D-GLDPC C_1	D-GLDPC A_1
SVNs			
(2,1) RC	0.3	0.28	0.6
(3,1) RC		0.12	0.05
(4,1) RC	0.2	0.05	0.05
(9,8) SPC	0.5	0.55	0.3
SCNs			
(6,5) SPC	0.09	0.1	0.13
$(3, 2)^2$ SPC-PC	0.91	0.9	0.87
Threshold (dB)	0.141	0.141	0.141

Fig. 7. EXIT chart for D-GLDPC code S_1 Fig. 8. EXIT chart for D-GLDPC code C_1 Fig. 9. EXIT chart for D-GLDPC code A_1

analyze the convergence behavior of decoders. Simulation results concluded that D-GLDPC codes with C -form SPC codes as SVN have the best stability and minimum decoding threshold, followed by D-GLDPC codes with S -form SPC codes as SVN, and the worst one is D-GLDPC codes with A -form SPC codes as SVN.

APPENDIX

PROOF $P_i^{-1}(x)$ IN A FORM AND x INTERSECT

We set

$$\begin{aligned} G(x) &= P_i^A(x) - x \\ &= \frac{(n_i - 1)(n_i - 2)}{n_i} x^2 \\ &\quad + \frac{2(n_i - 1)}{n_i} x^{n_i - 2} - x \end{aligned} \quad (15)$$

For $G(x)$, solving its first-order derivative, we obtain

$$\begin{aligned} G'(x) &= \frac{2(n_i - 1)(n_i - 2)}{n_i} x \\ &\quad + \frac{2(n_i - 1)(n_i - 2)}{n_i} x^{n_i - 3} - 1 \end{aligned} \quad (16)$$

From $G'(x)$, we are not able to observe its monotonic property, so we should continue to solve the second derivative $G''(x)$.

$$\begin{aligned} G''(x) &= \frac{2(n_i - 1)(n_i - 2)}{n_i} \\ &\quad + \frac{2(n_i - 1)(n_i - 2)(n_i - 3)}{n_i} x^{n_i - 4} \end{aligned} \quad (17)$$

By observing $G''(x)$, we know $G''(x) > 0$ when $0 < x < 1$ and $n_i > 3$. So $G'(x)$ is a monotonically increasing function. Therefore

$$G'(0) = -1 \quad (18)$$

$$G'(1) > 0 \quad (19)$$

We draw a conclusion that there must exist $\alpha \in (0, 1)$, such that $G'(\alpha) = 0$. So when $x \in (0, \alpha)$, $G(x)$ is a monotonically decreasing function; when $x \in (\alpha, 1)$, $G(x)$ is a monotonically increasing function. Since

$$G(0) = 0 \quad (20)$$

$$G(1) > 0 \quad (21)$$

there must be a $x \in (0, 1)$, which makes $G(x) = 0$, i.e., $P_i^A(x) = x$. This shows that $P_i^A(x)$ and x intersect, which is similar to that $P_i^{-1}(x)$ in A form and x intersect.

ACKNOWLEDGEMENT

This work was supported in part by the National Natural Science Foundation of China under Grants No. 61372077, No. 60972037, the Fundamental Research Program of Shenzhen City under Grants No. JC201005250067A and No. JCJY20120817163755061.

REFERENCES

- [1] R. G. Gallager, "Low-density parity-check codes," *IRE Trans. Inform. Theory*, vol. 8, pp.21-28, Jan. 1962.
- [2] D. J. C. MacKay and R. M. Neal, "Near Shannon limit performance of low density parity check codes," *Electron. Lett.*, vol. 32, no. 8, pp. 1645-1646, 1996.
- [3] M. Luby, M. Mitzenmacher, A. Shokrollahi, and D. Spielman, "Analysis of low-density codes and improved designs using irregular graphs," in *Proc. ACM Symp. Theory Comp.*, Dallas, TX, 1998, pp. 249-258.
- [4] Yige Wang and Marc Fossorier, "Doubly Generalized LDPC Codes," in *Proc. IEEE International Symposium on Information Theory*, 2006, pp. 669-673.
- [5] R. M. Tanner, "A recursive approach to low complexity codes," *IEEE Trans. Inf. Theory*, vol. IT-27, no. 5, pp. 533-547, Sept. 1981.
- [6] M. Lentmaier and K. Zigangirov, "On generalized low-density parity-check codes based on Hamming component codes," *IEEE Commun. Letters*, vol. 3, no. 8, pp. 248-250, Aug. 1999.
- [7] J. Boutros, O. Pothier, and G. Zemor, "Generalized low density (Tanner) codes," in *Proc. IEEE. Int. Conf. Commun. (ICC'99)*, vol. 1, Jun. 1999, pp. 441-445.
- [8] G. Yue, L. Ping, and X. Wang, "Generalized low-density parity-check codes based on Hadamard constraints," *IEEE Trans. Inf. Theor.*, vol. 53, no. 3, pp.1058-1079, Mar. 2007.
- [9] Yige Wang and M. Fossorier, "EXIT chart analysis for doubly generalized LDPC codes," in *Proc. 2006 IEEE Global Telecommunications Conf.* San Francisco, CA, Nov. 2006, pp. 1-6.
- [10] Yejun He, Guiyuan Sun, Jie Yang, and Francis C. M. Lau, "D-GLDPC Codes with 3-D Single Parity-Check Product Codes as Super Check Nodes," in *Proc. 2014 IEEE International Conference on Wireless Communications and Signal Processing (WCSP2014)*, Hefei, China, Oct. 2014.
- [11] T. Richardson and R. Urbanke, "Modern Coding Theory," 2007 [Online]. Available: <http://lthwww.epfl.ch/mct/index.php>, preprint.
- [12] E. Paolini, M. Fossorier, and M. Chiani, "Doubly-generalized LDPC codes: Stability bound over the BEC," *IEEE Trans. Inform. Theory*, vol. 55, no. 3, pp. 1027-1046, Mar. 2009.
- [13] A. Ashikhmin, G.Kramer, and S. ten Brink, "Extrinsic information transfer functions: Model and erasure channel properties," *IEEE Trans. Inform. Theory*, vol. 50, no. 4, pp. 1651-1672, Apr. 2010.
- [14] E. Sharon, A. Ashikhmin, and S. Litsyn, "EXIT functions for binary input memoryless symmetric channels," *IEEE Trans. on Commun.*, vol. 54, no. 7, pp. 1207-1214, Jul. 2006.
- [15] D. M. Rankin and T. A. Gulliver, "Single parity check product codes," *IEEE Trans. on Commun.*, vol. 49, no. 8, pp. 1354-1362, Aug. 2001.